Title

Interface mechanics of carbon fibers with radially-grown carbon nanotubes

Authors

Subramanian, Nithya

Koo, Bonsung

Venkatesan, Karthik Rajan

et al.

Publication Date

2018-08-01

DOI

10.1016/j.carbon.2018.03.090

Carbon 134 (2018) 123–133

Contents lists available at ScienceDirect

Carbon

journal homepage: www.elsevier.com/locate/carbon

Interface mechanics of carbon fibers with radially-grown carbon nanotubes

Nithya Subramanian, Bonsung Koo, Karthik Rajan Venkatesan, Aditi Chattopadhyay*

Arizona State University, 551 E. Tyler Mall, Tempe, AZ, 85287, USA

ARTICLE INFO

Article history:
Received 2 February 2018
Received in revised form
27 March 2018
Accepted 29 March 2018
Available online 31 March 2018

ABSTRACT

An atomistic modeling framework to investigate the interface/interphase of composite architecture with carbon fibers containing radially-grown carbon nanotubes (often called fuzzy fibers) is detailed in this paper. A polymeric functional coating for the carbon fiber surface, which also serves as a substrate for the CNT growth, is explicitly modeled. The tensile and transverse moduli of the fuzzy fiber/epoxy interphase is computed from virtual deformation simulations and compared to experimental values reported in literature, in order to validate the nanoscale model. Furthermore, the effect of the polymer substrate is studied by modeling the local interphase mechanics. Various modes of virtual loading provide the cohesive behavior of the local substrate/epoxy interphase. Conclusions are presented by comparing the material response of the interphase with and without the polymeric substrate. The integration of results from the nanoscale to an atomistically-informed subcell-based continuum level model is also demonstrated in the paper.

1. Introduction

The potential of nanocomposites for mechanical, thermal, electrical, and biological applications has been widely researched. With computational models serving as guidelines for material design, novel nanomaterials with improved functionalities can be designed and synthetized with atomic-scale precision, opening new frontiers in nanotechnology. The exceptional properties of carbon nanotube (CNT) nanocomposites, in particular, can be truly leveraged by being able to carefully control the parameters for their synthesis, resulting in specific, high-precision morphology and architecture. The stress non-homogeneity introduced by the dispersion of CNTs in fiber reinforced polymer matrix composites (PMC) is governed by the morphology of the CNT network. Results from the computational studies presented in literature elucidate that conventional strategies for the introduction of CNTs in fiber reinforced PMC, such as CNT dispersion in the matrix improve the elastic-plastic response [1], fracture toughness [2,3], and stiffen the fiber/matrix interphase by providing an alternate load path under debonding [4]. However, studies have also shown that local agglomeration of CNTs cause microscopic stress concentrations in the matrix zones and lead to early damage [5,6]. Selective reinforcement of matrix zones has been attempted by adding CNTs as "bridges" to inter-fiber areas to cause crack arrest. Although the study showed more homogenized spatial distribution of stress values and delay in damage initiation, the results are highly sensitive to the direction of applied load. Furthermore, the authors concede that the practical realization of complex nanoparticle arrangements rely significantly on advancements in the principles of directed self-assembly of nanoparticles [7].

Researchers are also investigating specific nanoarchitectures for CNT growth that yields specific performance gains in predetermined loading and service conditions. The choice of the types and arrangements of CNTs extends the potential design space, resulting in tunable material behavior. Various architectures such as CNT fuzzy fibers, CNT ropes and CNT tapes are being explored for potential applications to light-weight airframe structures [8–10]. Qian et al. studied the nature of load transfer in a single walled CNT bundle consisting of seven (10, 10) CNTs using molecular mechanics (MM) and molecular dynamics (MD). They found that the surface tension and the inter-tube corrugation contributed to load transfer in the parallel bundle and the twisting of nanotubes in the bundle system could significantly enhance the load transfer [11]. Due to strong van der Waals interactions between CNTs, predefined architectures could prove to be game-changing in the transfer of their excellent nanoscale properties

* Corresponding author.
E-mail address: aditi@asu.edu (A. Chattopadhyay).

https://doi.org/10.1016/j.carbon.2018.03.090
0008-6223/

to bulk structure. However, the successful optimization of such architectures with significantly improved performance metrics still remains a challenging endeavor. Supplementary to empirical and synthesis efforts, computational approaches can provide a means to investigate potential carbon nanotube structures, indicating possible systems and configurations that warrant experimental and physical realization.

The fuzzy fiber architecture contains a microfiber core, made of carbon, glass, ceramic or alumina, coated with radially oriented CNTs prior to matrix impregnation. The fiber in itself is hierarchical, and fuzzy fiber composites are shown to have enhanced mode-I fracture toughness, interlaminar shear strength, thermal and electrical properties. However, researchers have observed a trade-off between high-yield CNT growth on the fiber, and the tensile properties of the carbon fiber, which is critical to the in-plane response of composites. In order to produce circumferential CNT growth without degrading fiber properties, a catalyst adhesion that does not damage fiber exteriors was explored. A polymeric functional coating with Poly(styrene-*alt*-dipotassium-maleate) (K-PSMA) for carbon fiber with radial CNTs resulted in a fuzzy fiber composite that maintained its in-plane properties in comparison to baseline fiber reinforced PMCs.

Several studies have been carried out to investigate the effective properties of fuzzy fiber composites based on nanomechanics and homogenization approaches [12–15], effective thermoelastic properties using the Mori-Tanaka approach [16], piezoresistive behavior using a 3D computational micromechanics model within an FE framework [17]. These studies consider CNTs to be perfectly straight radial structural elements with a uniform density of growth. The inclusion of stochasticity becomes difficult in these models and deterministic outputs show significant discrepancies, especially for complex nanoarchitectures. Kundalwal and Ray implemented sinusoidal functions (with wavelength and angle as variables) to capture the waviness of the CNTs and its effects on the coefficient of thermal expansion (CTE). Their analytical constitutive model showed an improvement in CTE for wavy CNT fuzzy fibers [18]. However, these micromechanics approaches do not yield accurate estimates for interfacial interactions and post-elastic behavior; the experimental validations provided for the results from micromechanics models are also limited to elastic material property comparisons. To date, a holistic atomistically-informed model of the fuzzy fiber accounting for intermolecular interactions, including the polymeric functional coating has not been explored to the best of the authors' knowledge.

The atomistic modeling of the fuzzy fiber nanocomposite architecture including the functional coating and its critical interphases is presented in this paper. The mechanical properties of the nanocomposite interface are evaluated through virtual deformation simulations, and the effect of the PSMA coating is quantified by formulating atomistically-informed cohesive law for the interface. There is an abundance of experimental data, both at the micro level (single fiber tests) and at the meso level (nanocomposite tests), for this architecture. This wealth of reported literature from micromechanics modeling and experimental sources provide a valuable opportunity to explore the implementation and necessity of an atomistically-informed computational framework for specific nanoengineered architectures. Furthermore, the performance and property gains (and losses) from the fuzzy fiber architecture are compared with nanocomposites containing dispersed CNTs. Potential suggestions for improving the design of the architecture, acquired from the simulations, are provided.

2. Fuzzy fiber nanocomposites modeling for mechanical properties

2.1. Fiber surface coating

In the experimental studies that focused on the growth of CNTs directly on the carbon fiber or the carbon fiber cloth, various fiber coatings were used to improve quality of growth and resulting properties. These coatings could be polymeric (e.g. polyvinyl alcohol [19], PSMA) or ionic (e.g. ferrocene [20]), and led to denser packing of CNTs on the carbon fiber surface. In this subsection, the atomistic modeling of a polymeric functional coating material – PSMA, is introduced. Although the emphasis here is to model all constituent phases in the fuzzy fiber nanocomposite, the ion exchange processes on the carbon fiber surface and the by-products from catalytic chemical vapor depositions processes that results in the growth of the CNTs are not included in this simulation. PSMA is a thermoplastic polymer built up of styrene maleic anhydride monomers – the chemical structure which is shown in Fig. 1 (a). The polymerization process results in a chain of repeating monomers, and a schematic of a chain with eight monomer units is presented in Fig. 1 (b).

The chemical and topological structures of PSMA were generated using an open-source package called Open Babel [21] for 3D molecular co-ordinates, and the force field parameters were created via an open-source platform from Swiss Institute of Bioinformatics [22]. The force field parameters were generated based on the MMFF potential after careful considerations of its usability for organic thermoplastic polymers. It is important to note that the PSMA chain was not generated by explicitly simulating the polymerization process. Instead, a chain connecting monomers were generated and the MMFF force field parameters for the polymer chain were directly included in the simulations. This is justified because the polymerization process of PSMA is not relevant to the growth or the behavior of CNTs. In the physical experiments, the coating material consists of the polymer that is the end result of the polymerization process; therefore, the simulation of polymerization is found to be outside the scope of this study. PSMA, subsequent to the polymerization process, is included in the atomistic model on the fuzzy fiber interface.

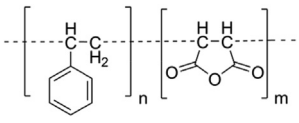

(a)

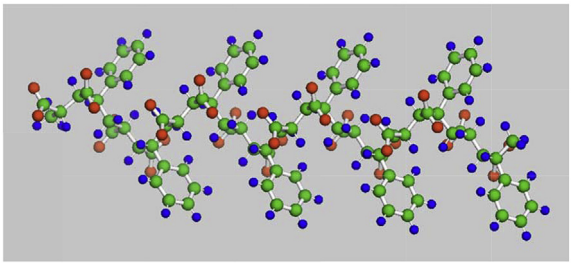

(b)

Fig. 1. (a) Chemical structure of styrene maleic anhydride monomer; (b) Schematic of PSMA polymer chain with eight monomer units.

2.2. Model set-up

The fuzzy fiber nanocomposite model at the nano scale is orginally comprised of five constituents: carbon fiber surface, polymeric functional coating, radially-grown CNTs, the epoxy resin, and the hardener. A schematic, in Fig. 2, illustrates the nanocomposite with ideal and uniform CNT growth and fiber arrangement, where the pale yellow represents the epoxy matrix in which the fuzzy fibers are embedded.

The nanoscale simulation volume is generated using PackMol [23] with some modification which allows creating large system size (>100,000 atoms). The carbon fiber surface is represented by void-induced, irregularly-stacked, graphene layers to simulate surface roughness; the graphene layers are also saturated with hydrogen for thermal stability, as detailed in Ref. [24]. Four radially-grown CNTs of chirality (10, 10) are embedded in the PSMA chains; they are physically dispersed with no functionalization. The epoxy phase consists of DGEBF (Di-Glycidyl Ether of Bisphenol F) resin and DETA (Di-Ethylene Tri-Amine) hardener molecule, prior to crosslink formation, dispersed randomly in the unit cell inside a predefined box. The unit cell generated from PackMol is shown in Fig. 3. The unit cell dimensions are $40 \times 45 \times 35\ nm^3$; however, the y- and z-directional dimensions are not of critical relevance due to periodic boundary conditions (PBC) imposed in simulations. The model, currently with over 200,000 atoms, can be easily modified to adjust CNT height and density, fiber surface roughness, and PSMA coating thickness.

The MD simulations for the fuzzy fiber nanocomposite are performed with hybrid classical force fields, initially. The crystalline CNT and graphene molecules utilize the Optimized Potential for Liquid Simulations – All Atom (OPLS-AA) [25] and the Consistent Valence Force Field (CVFF) [26], whereas the thermoplastic PSMA chains and the thermoset polymer use the Merck Molecular Force Field (MMFF) [27]. The simulations implement PBC along the y- and z-directions. However, PBC are not appropriate along the x-direction, as shown in Fig. 3, due to the phase discontinuity that arises if the unit cell were to be repeated infinitely in that direction.

2.3. Crosslinking and equilibration

Prior to crosslinking of the epoxy, an energy minimization of the unit cell is performed using the conjugate gradient approach. Subsequently, equilibration is performed under an NPT (isobaric-isothermal) ensemble at 300 K and 1 atm for 30 ns (1fs time step) using the Nose-Hoover thermostat and barostat. During equilibration, the potential energy of the unit cell converges to a mean value with minimal variance, which is considered to be the initial, equilibrated state. It is also important to note that although the graphene layers are stacked in an ordered fashion during packing,

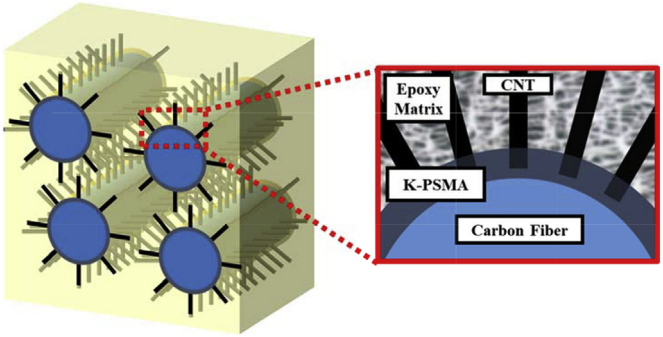

Fig. 2. Ideal fuzzy fiber nanocomposite and interface.

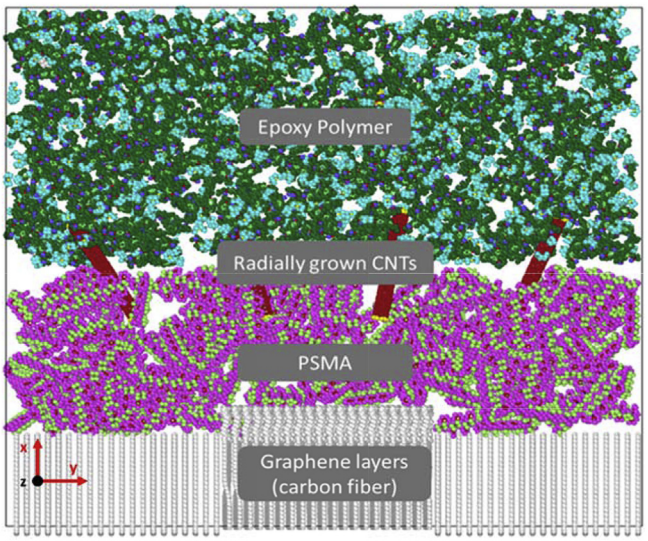

Fig. 3. Fuzzy fiber nanocomposite unit cell generated from PackMol.

the equilibration creates an irregular sequence of layers based on their molecular interactions. This is useful in representing/modeling the inherent peaks and valleys present on the fiber surface. Subsequent to the equilibration, the epoxy resin and hardener molecules are numerically crosslinked using the cut-off distance based approach described in Ref. [28].

During the numerical crosslinking simulation, an NVT ensemble equilibration (at 300 K, 1 atm, for 1000 ps) is performed to promote the intermixing of molecules; this creates proximity between the active sites leading to new bond formation. A cut-off distance of 4 Å was used, which is equivalent to van der Waals radii between carbon (active sites of resin) and nitrogen (active sites of hardener) atoms. The crosslinking degree/conversion degree of the epoxy phase is calculated based on the number of new bonds formed and the total number of potential bonds between the active sites. Fifty simulations were performed on the fuzzy fiber nanocomposite to evaluate the mean conversion degree. The result, as seen Fig. 4, is a non-smooth normal distribution, (more simulations could smoothen the distribution) with a mean of 37.12% and a standard deviation of 0.73%. Although the mean conversion degree of neat epoxy is about 56%, as seen in Ref. [28], the CNTs that protrude into the epoxy phase act as a barrier for their crosslinking. In the current

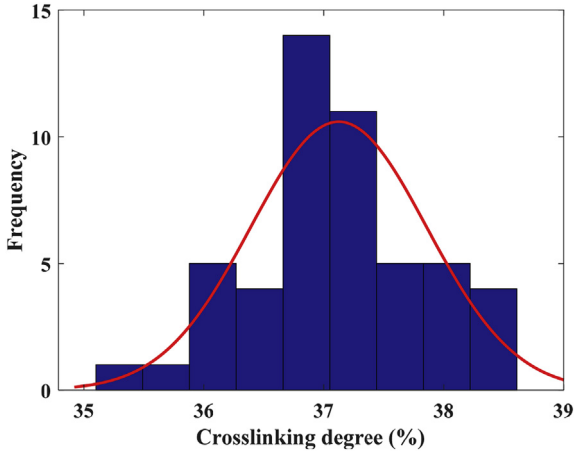

Fig. 4. Distribution of crosslinking degree for epoxy in fuzzy fiber nanocomposite.

configuration, the CNT weight fraction is over 5%. Since, the CNTs are arranged at the edge of the epoxy phase instead of being randomly dispersed in the midst of the epoxy molecules, the crosslinking is not significantly impeded.

2.4. Boundary and loading conditions

The unit cell is subjected to virtual deformation simulations along the x-, y- and z-directions. Prior to the deformation test, an NPT equilibration is performed for 10 ns to remove stresses from the molecular system, while the temperature is maintained at 300 K. The virtual deformation tests are performed on the fuzzy fiber nanocomposite using ReaxFF force fields with the specific parameter set from Singh et al. [29]. The pair energy difference of the fuzzy fiber nanocomposite system at the beginning and at the end of equilibration was calculated using classical and reactive force fields, and were matched to a tolerance of 1×10^{-2} kCal/mol. This ensures the validity of the choice of reactive potential parameters because the energy from van der Waals interactions are calculated using similar formulations in both classical and reactive force fields.

As demonstrated in Fig. 5 (b) and (c), the 'fix deform' command is used to apply a tensile load to the simulation box causing the atoms to be remapped based on an affine transformation, along the y- and z-directions, respectively. An NPT equilibration is performed during the tensile deformation to control the temperature. Since the simulation volume is non-periodic along the x-direction, a region of atoms in the graphene layer is constrained, and a region of atoms in the epoxy phase is moved with a constant velocity in the x-direction (as illustrated in Fig. 5 (a)) using the 'fix_move' command. The atoms that are not part of these two regions are allowed to move freely based on the local atomic forces acting on them; this is implemented using the 'fix_move NULL' command. A Berendesen thermostat is also employed in conjunction with the 'fix_move' commands to monitor and maintain the temperature of the fuzzy fiber molecular system.

3. Results of virtual deformation simulations

The virtual deformation along the x-direction (Fig. 5) is performed by displacing a region of epoxy polymer at the interphase; Johnston et al. [30] performed MD simulations of the fiber/matrix interphase and obtained elastic properties to incorporate into a subcell-based micromechanics model. The authors concluded that displacing a portion of the polymer region, as opposed to the entire polymer phase, yields a better estimate of the tensile and transverse moduli. The loads leading to material failure originate away from the interphase, and are transferred to the constituents at the interphase through the physical and chemical links; thus, displacing a portion of the polymer captures the load transfer mechanisms through the polymer chains and entanglements. Fig. 6 illustrates the smoothed stress-strain response from the x-directional deformation of the fuzzy fiber nanocomposite. The modulus obtained from the elastic region of the stress-strain data set corresponds to the transverse modulus of the fuzzy fiber/matrix interface, with a value of 15.45 GPa. A tabular comparison of transverse moduli

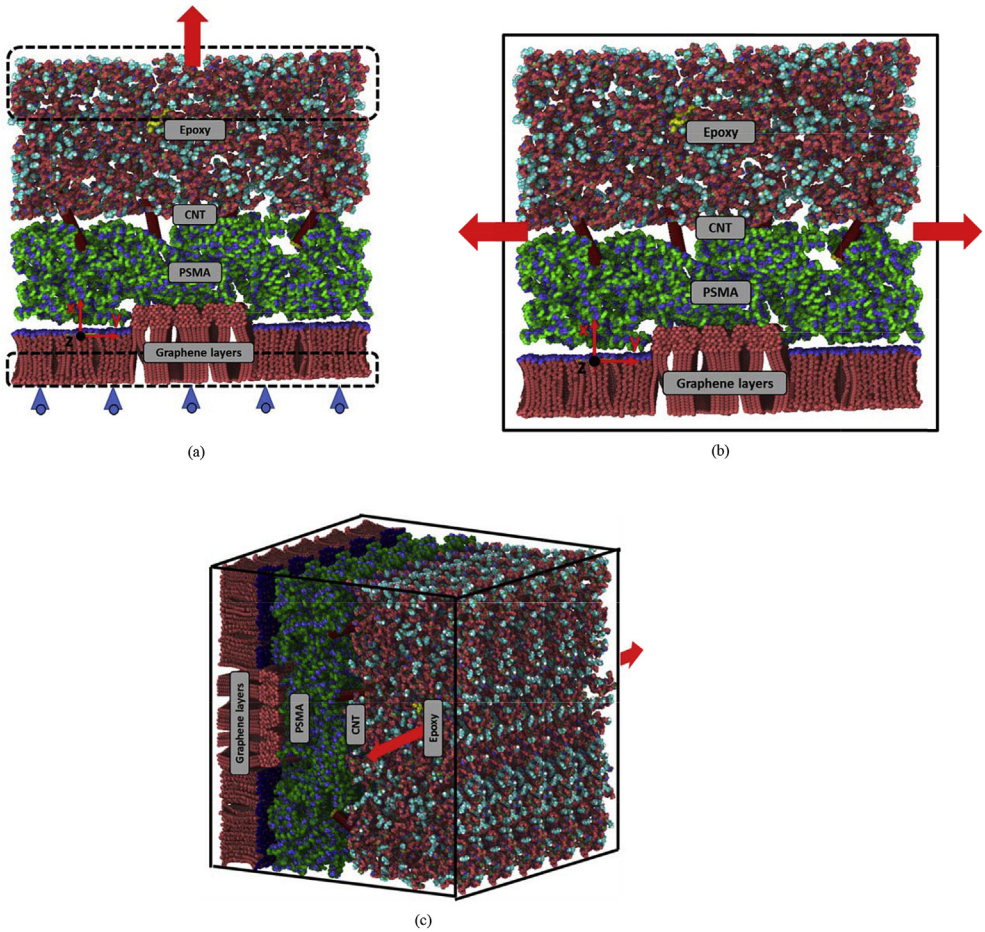

Fig. 5. Loading of Fuzzy Fiber Nanocomposite along (a) x-direction; (b) y-direction; (c) z-direction.

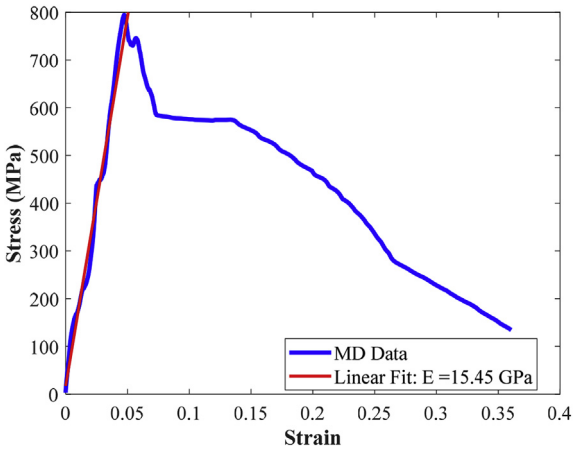

Fig. 6. Stress-Strain Curve from Deformation along x-direction.

presented in Ref. [30] ranges from 3.37 GPa to 34 GPa estimated through various micromechanics models. The transverse modulus calculated by Johnston et al. from their molecular simulations is 8.28 GPa for a neat fiber/matrix interface. In comparison, the transverse in-plane modulus of the fuzzy fiber/matrix interface shows an improvement at 15.45 GPa. This improvement is attributed to the orientation of the CNTs along the debond direction, thus leading to an efficient load sharing mechanism, even as the polymer fails. The initial load-drop at ~7% strain corresponds to the failure of the polymer chains; the load is subsequently transferred to the CNTs, the graphene layers and the PSMA layer, thus, leading to a slow deterioration of the interface, instead of a sudden failure and load-drop. Fig. 7 plots the cumulative bond dissociation energy (BDE) during the x-directional deformation. The variation of bond energy between the undeformed, unbound state of the molecular system and at each timestep of the deformation test is used to quantify the bond dissociation energy. It is important to note that the BDE is affected predominantly by the polymer chains due to the presence of weak as well as strong bonds. The increase in BDE up to a strain of ~7% indicates the scission of weak polymer bonds; the bonds in the CNTs and the graphene layers are relatively too strong to be broken under this loading. Therefore, subsequent to the failure of the polymer matrix, the slope of the BDE curve drastically reduces. The gradual increase in the BDE curve beyond 10% strain could be attributed to the cleaving of bonds in the PSMA layer. It is worth mentioning that the absolute value of tensile transverse strength, ~745 MPa as inferred from Fig. 6, is overestimated by MD simulations. Although functional trends (and therefore modulus estimates) are accurately obtained from MD, the value of stress itself is often overestimated due to the high strain rate simulations.

The stress-strain and BDE results from y-directional (relative shear-induced out-of-plane) deformation are plotted in Fig. 8 and Fig. 9, respectively. The out-of-plane modulus of the interphase is found to be 10.4 GPa, and compares well with the transverse modulus for the fiber/matrix interface found in literature (~10–13 GPa) [31]. Note that for a typical fiber/matrix interface, the transverse moduli along x- and y-directions (as defined in this study) are assumed equal. Since the CNTs are transversely aligned to the loading direction, their effect on the transverse modulus is expected to be negligible. Thus, the transverse modulus value from this study (10.4 GPa) compares well with the value of 8.28 GPa for the fiber/matrix interface from Ref. [30]. Furthermore, the transverse modulus of fuzzy fiber composites was calculated by Rafiee to be 10.00± 1.36 GPa using an elaborate effective property approach with stochastic effects, and the value from the current model compares perfectly [32]. There is a clear yield point, followed by a softening and a hardening phenomenon in Fig. 8. The strain softening occurs due to the failure of the polymer chains; the stress drops as the polymer chains break in quick succession. The strain hardening occurs when CNTs, upon polymer failure, orient themselves along the loading direction in the newly generated voids. The reorientation of the CNTs causes a hardening phenomenon with a slope almost as steep as the slope of the elastic region. Unlike traditional fiber/matrix composite interfaces that have equal moduli along the two transverse directions (x and y), the fuzzy fiber/matrix interface has a higher transverse modulus along the direction of the CNTs (x). The y-direction in this model, being also transverse to the orientation of the CNTs, has a lower modulus. In Fig. 7, the BDE curve was bilinear due to the polymer phase failing first followed by the transfer of load to the other constituent phases. However, the BDE curve along the y-direction (see Fig. 9) is smooth because all the phases are deformed simultaneously. The combination of polymer chains breaking in the PSMA and the epoxy thermoset phases creates a smooth BDE curve. It is worth noting that as complete material failure occurs, the saturated BDE value (~14,000 kCal/mol) is quite comparable along the x- and y-directions.

The results from the virtual deformation along the fuzzy fiber direction are presented in Fig. 10 and Fig. 11. The longitudinal modulus of the fuzzy fiber/matrix interface is calculated to be 17.32 GPa from Fig. 10; note that along this direction, the infinitely

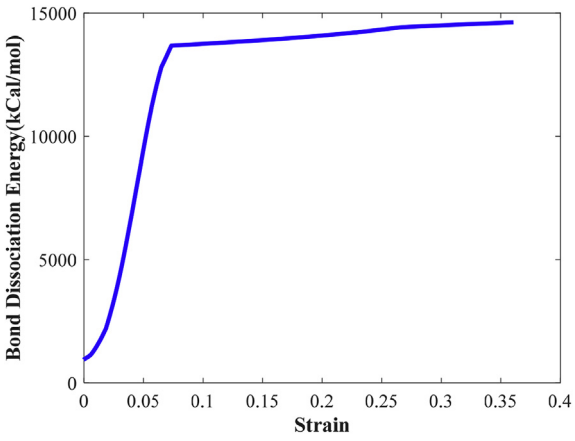

Fig. 7. BDE Curve from Deformation along x-direction.

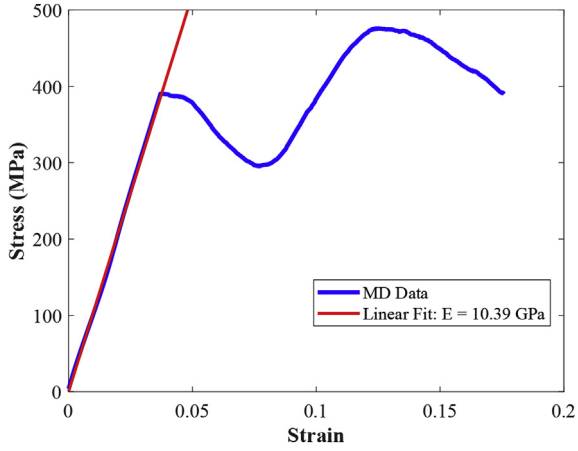

Fig. 8. Stress-Strain Curve from Deformation along y-direction.

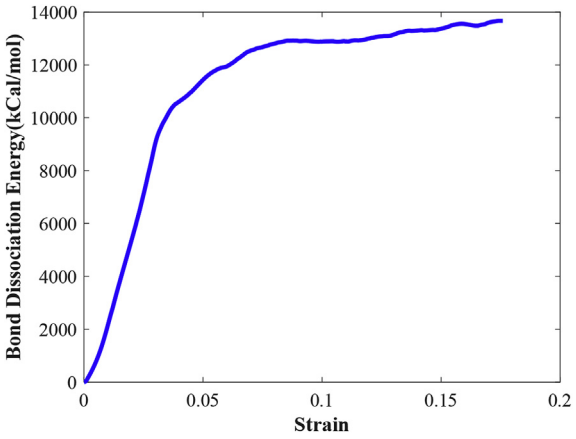

Fig. 9. BDE Curve from Deformation along y-direction.

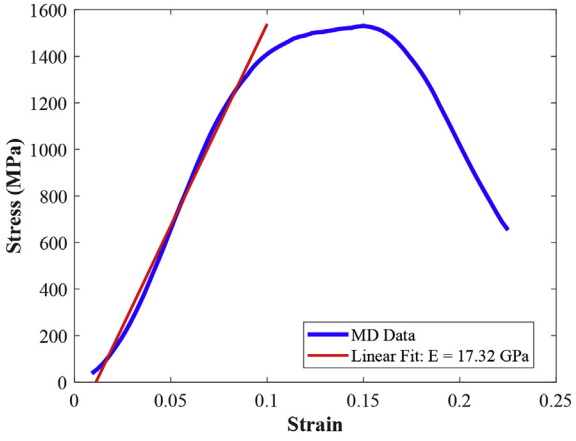

Fig. 10. Stress-Strain Curve from Deformation along z-direction.

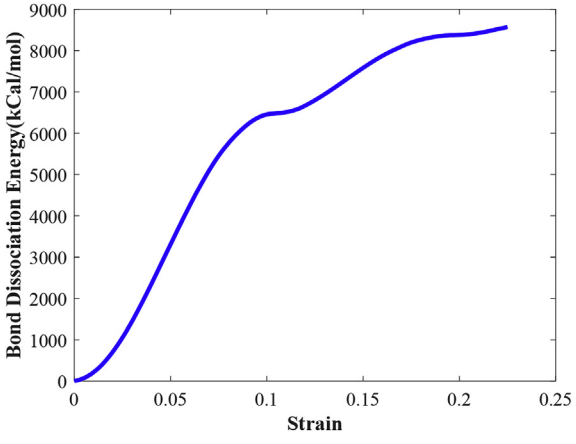

Fig. 11. BDE Curve from Deformation along z-direction.

long graphene layers (due to periodic boundary conditions along z) act as dominant load carrying constituents. A fairly large elastic region (~7% strain) and the absence of a softening mechanism indicating polymer failure, attest to the load carrying role of the graphene layers. The modulus is therefore, higher than the x- and the y-directions. The values of longitudinal moduli in literature for fuzzy fiber nanocomposites calculated from Mori-Tanaka and concentric cylinders based approaches tend to be much higher ranging from ~50 GPa [12] to ~150 GPa [32]. Furthermore, there are no explicitly reported properties for the fuzzy fiber interface since the models assume material properties for the individual constituents such as CNT, epoxy and carbon fiber. This model, however, only simulates the external surface of the fiber through graphene layers, which corresponds to a low fiber volume fraction (vf) value at the continuum level. Therefore, the longitudinal modulus of the fuzzy fiber nanocomposite interface can only be compared to rule-of-mixtures estimates that are obtained with low fiber volume fraction assumptions for the interface. The BDE curve in Fig. 11 exhibits a trend different from a matrix-dominated damage mechanism. The BDE is not fully saturated at ~20% strain, indicating that complete polymer failure has not occurred, and further proved by the fact that the value of maximum BDE (~9000 kCal/mol) is also significantly lower than in the x- and y-directions.

During the tensile deformation simulations described above, the Poisson's effect is accounted for in our simulation by maintaining stress-free boundary conditions on the two faces that are not being deformed (under uniaxial tension). This is performed in MD simulations by equilibrating the unit cell under NPT ensemble with 0 atm, pressure along those two directions (not being deformed). The shear moduli were obtained from explicit shear simulations on the unit cell. It is to be noted that shear deformations were performed along xy, xz, yz, and also along yz, zx, and zy. This is because shear deformation response along xy and yx are not equivalent in amorphous non-homogeneous material systems. The averaged shear moduli values were estimated to be 2.35, 3.16, and 4.58 GPa along xy, yz, and xz, respectively. The elastic properties for the fuzzy fiber/matrix interface obtained from reactive MD simulations are incorporated into a high fidelity generalized method of cells (HFGMC) based micromechanics model to investigate the mechanical properties of a unidirectional fuzzy fiber composite. The HFGMC model yields improved accuracy by employing a second-order subcell displacement field. This enables shear coupling between subcells, which can capture the effect of interphase on the nanocomposite response. The microvariables in the higher-order (second-order) displacement field for each subcell are solved through the assignment of equilibrium, boundary, and traction continuity conditions imposed in an averaged form. The details of the formulation and subcell configuration of HFGMC are provided in our previous work [30]. The micro scale repeating unit cell (RUC) is defined by a continuous fiber inclusion in the y1-direction and is assumed to be periodically distributed in the y2-y3 plane. The relationship between the MD unit cell and HFGMC interphase subcell is defined by a transformation of the compliance matrix corresponding to the radial angle of CNT growth. A comparison of results from the micromechanical model with available experimental data for fuzzy fiber composites and traditional fiber reinforced composites is presented in Table 1. The tabulated values serve to not only validate the current model but also to compare the properties of the fuzzy fiber architecture to traditional fiber reinforced composites. It is also important to note that experimental data for tensile and transverse moduli were available for two different fiber volume fractions from two separate sources; hence the HFGMC analysis is performed at 40% and 70% to ensure consistent comparison. The comparison of the obtained transverse modulus of fuzzy fiber composite yields a 31.7% improvement with respect to traditional fiber reinforced composites. The obtained values of tensile and transverse moduli from the HFGMC model for the unidirectional fuzzy fiber composite and traditional fiber reinforced composite are in good agreement with the experimental observations.

Data from literature on an effective fiber approach [32] reported 11.2 GPa as the transverse modulus for ~40% fiber volume fraction. Although this compares well with the experiments and the current

Table 1
Comparision between experimental data and atomistically-informed HFGMC model.

	Atomistically-informed HFGMC		Experimental data	
	E_{11} (GPa) at 70% vf	E_{22} (GPa) at 40% vf	E_{11} (GPa) at 70% vf	E_{22} (GPa) at 40% vf
Fuzzy fiber composite	189.32	10.8	203 ± 7.6 [33]	10.2 ± 1.3 [34]
Fiber reinforced composite	187	8.2	198.3 ± 5.0 [33]	7.8 ± 1.09 [35]

model, the suitability of effective property approaches is limited to investigating the effective elastic response. The present computational framework is capable of modeling the localized response rather than the homogenized properties; it can further be extended to investigate nonlinear behavior and damage mechanisms through atomistically-informed physics-based damage models.

3.1. Modeling interface/interphase mechanics

This section presents the studies conducted to isolate the effects of the PSMA coating on the interface mechanics of the nano-engineered composite. Previously, it is observed that the PSMA coating affects the out-of-plane transverse modulus significantly. In order to quantify the influence of the PSMA coating, the local outer interphase is modeled separately. This local interphase consists of the PSMA substrate and the epoxy polymer phase with CNTs grown on the substrate protruding in to the epoxy, as depicted in Fig. 12. The construction of the unit cell using PackMol involved randomly dispersing PSMA and epoxy molecules in adjacent boxed regions. A CNT of chirality (10,10) is inserted in between the two phases. The x-direction of the local interphase model runs perpendicular to the boundary separating the two phases. This, once again, results in a non-periodic boundary along x, whereas y- and z-directions could be assumed to be periodic.

By analyzing this local interphase in Fig. 12, and comparing the cohesive behavior to the results presented in Ref. [24], important conclusions can be drawn about the difference in mechanics between the carbon fiber/matrix interface and the fuzzy fiber/matrix interface. To ensure consistent comparison, the local interphase is subject to the same loading and boundary conditions – a debond mode by deforming the two phases apart from each other (along x), a relative shear-induced rotation along y, and a relative shear-pullout mode along z [24]. The system size is ~60,000 atoms in a box of dimensions $13 \times 10 \times 5\ nm^3$; the current model allows the entanglement of PSMA chains with the thermoset polymer chains during equilibration. However, the initial set up consists of the two phases clearly demarcated into two non-overlapping regions. The big question that serves as the motivation for this analysis is whether the inclusion of the polymeric coating improves (or degrades) interface properties and why. Another contention that needs to be settled is the trade-off between in-plane and out-of-plane response of the fuzzy fiber nanocomposite; several studies have reported a loss of in-plane transverse modulus, while showing a significant improvement in out-of-plane (interlaminar) strength. The local interphase model is expected to provide insight on whether specific modes of response are degraded while resulting in improvements elsewhere.

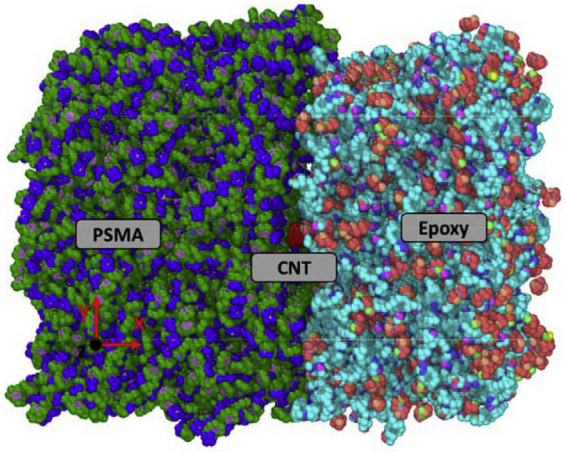

Fig. 12. Local interphase between PSMA coating and epoxy matrix.

After performing the numerical crosslinking simulation for the epoxy phase, virtual deformation simulations are performed on PSMA/epoxy interphase based on the boundary conditions and loads described in Fig. 5. During the deformation, equilibration is performed on the local interphase system under an NPT ensemble (300 K, 0 atm for stress-free boundaries); an added Berendsen thermostat is implemented to maintain the temperature around 300 K. The pullout along the x-direction corresponds to the matrix debond failure mode; the deformations along the y-direction and z-direction correspond to relative shear-induced out-of-plane rotation and in-plane pullout, respectively.

Fig. 13 depicts the variation of the cohesive force with x-directional displacement at the PSMA/epoxy interphase during matrix debond. The cohesive behavior is a unimodal smooth curve; the initial peak (depicted by a red dot) corresponds to the stretching of the epoxy polymer chains causing interphase separation. The final frame shows the separation of the interphase due to epoxy polymer chain breakage. It is interesting to note that the cohesive forces between the PSMA and epoxy polymer phase is stronger than the intermolecular forces in the polymer itself. In Ref. [24], a bimodal traction-separation curve was observed for the fiber/matrix interphase. It was explained that the second peak occurred due to the separation of physically-entangled polymer chains from the graphene voids. In this case, since there are no physical entanglements, the interphase strength is determined by the van der Waals forces between the two phases. It is also important to point out that the CNT embedded at the interphase acts as a significant load carrying constituent, and the polymer chains break prior to the failure of the interphase. A comparison of the maximum cohesive force presented in Ref. [24] (~3.5 nN) and Fig. 13 (~4.6 nN) shows that the PSMA/epoxy interphase has a higher value of peak load. This indicates that the polymer coating improves the mechanics of the local interphase under matrix debond failure mode. The growth of CNTs on the polymer coating/substrate improves the load carrying capacity of the interface along the transverse direction, and delays debond failure by preventing interface separation.

The interphase separation along the y-direction corresponds to the relative shear-induced rotation and subsequent failure; this failure mechanism is dominated by overcoming the intermolecular interactions between the two phases, since they are not physically entangled or chemically bonded. The resulting traction-separation behavior is trapezoidal as shown in Fig. 14. The red dot represents the cohesive force and displacement at which the van der Waals

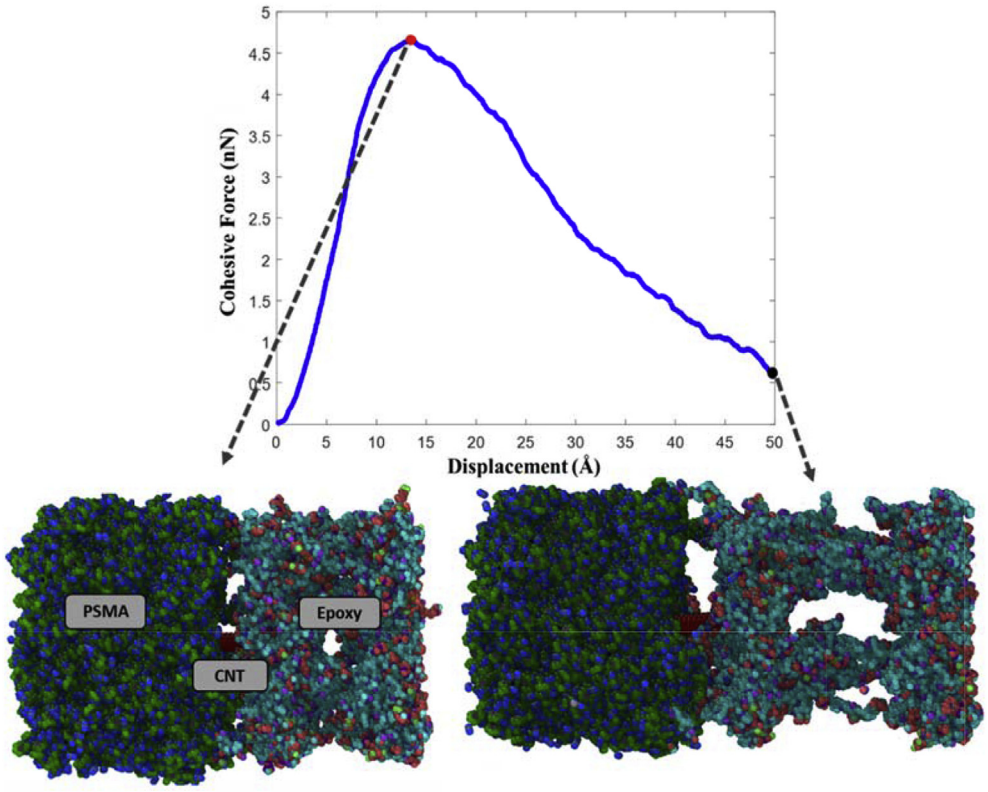

Fig. 13. Local Interphase (PSMA/Epoxy) Debond along x-direction.

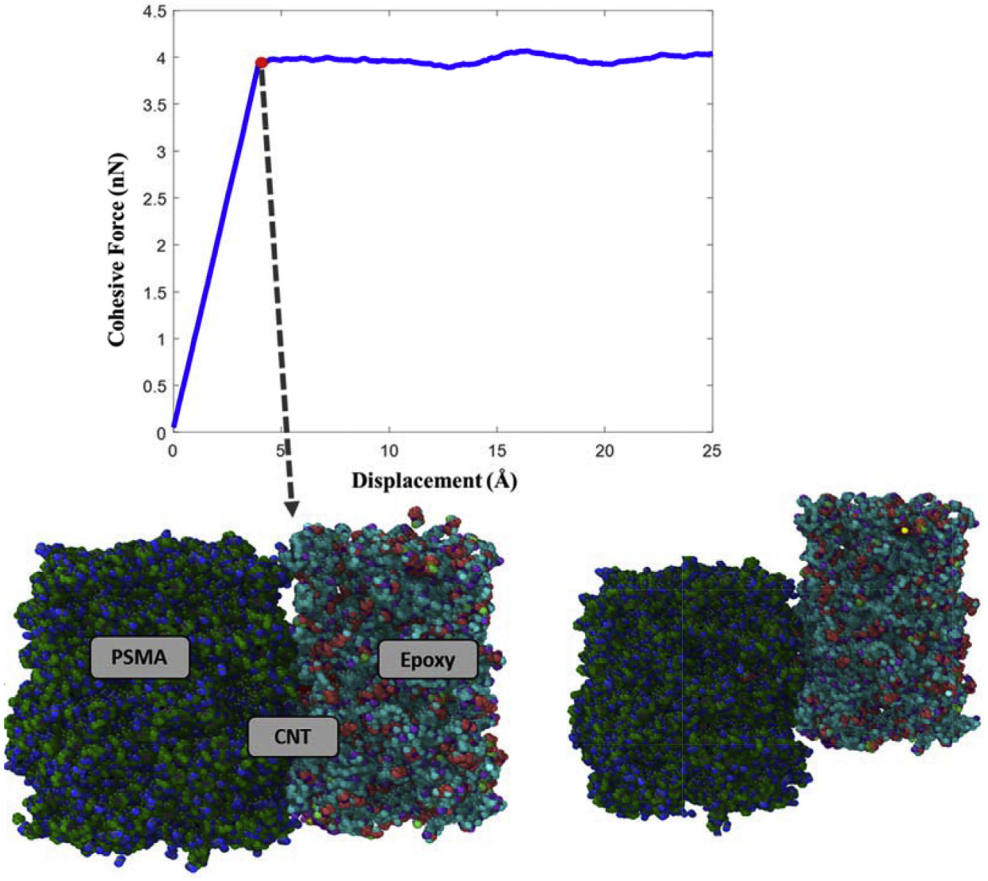

Fig. 14. Local Interphase (PSMA/Epoxy) Debond along y-direction.

forces are overcome, and the two phases start to slide past smoothly. The slight increase in resistance (higher cohesive force) around 15 Å is hypothesized to be due to the bending of CNTs as the polymer phase slides. The maximum cohesive force value of ~4 nN, along the y-direction, is higher than the value (~2.5 nN) observed in the fiber/matrix interphase [24]. This once again, leads to the conclusion that the out-of-plane properties show significant improvement with the introduction of the polymer coating between the fiber and the matrix. The final drop in load is not observed because the y-direction is periodic, and therefore, represents an infinitely long interphase.

The trapezoidal traction-separation behavior along the z-direction (seen in Fig. 15) is similar to the behavior along the y-direction. This is because the relative shear in these two phases is similar along both directions due to the dominant van der Waals's forces. The values of maximum cohesive force in Figs. 15 and 14 are comparable since the fiber is not explicitly modeled in this local interphase. As explained earlier, the slight increase in cohesive force beyond the red dot could be attributed to the resistance created by the bending of the CNT within the polymer as the two phases slide past each other. When the bending of the CNT is complete (~30 Å), the load is seen to drop gradually. The final drop in load is not observed due to the periodic boundary condition along the z-direction.

4. Conclusions

The significance of predetermined nanoengineered architectures were highlighted in this paper, in addition to the development of reliable computational tools that can accelerate the development of these architectures. Various CNT architectures such as nanoforests, CNT bundles and ropes, fuzzy fibers, etc. were reviewed, and their response under various loading conditions were compared based on data from reported literature. Among the CNT nanoarchitectures, a fuzzy fiber composite was chosen to demonstrate the versatility of the developed computational framework to investigate linear elastic behavior, damage mechanisms and interface mechanics, owing to the abundance of multiscale experimental results and micromechanics model predictions in literature.

An atomistic model of the fuzzy fiber nanocomposite was generated by explicitly modeling the various phases such as the carbon fiber, polymeric coating for the fiber surface, radially-grown CNTs, and the thermoset polymer matrix. Irregularly-stacked graphene layers with voids were included to represent the carbon fiber surface, and PSMA was chosen as the surface coating. Subsequent to the virtual curing of the epoxy phase, the fuzzy fiber model was deformed along the x-, y-, and z-directions to obtain the stress-strain response. Critical parameters such as the longitudinal and

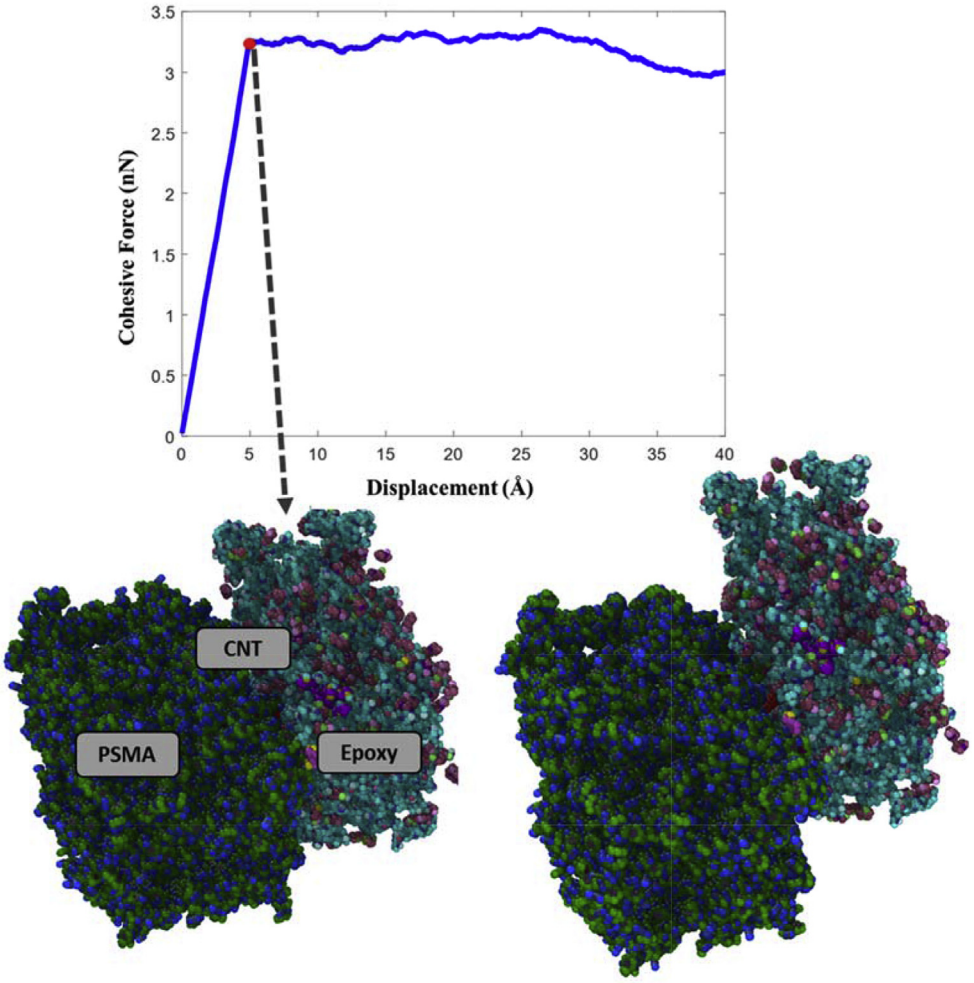

Fig. 15. Local Interphase (PSMA/Epoxy) Debond along z-direction.

transverse moduli were extracted from the results of the virtual deformation simulations. More importantly, the BDE variation was obtained as a function of strain, which provided insights into the unique damage mechanisms in these nanoengineered architectures along the different directions. The mechanism of load transfer was found to vary based on the direction of loading. Along the matrix debond direction (x-direction in the current model), the polymer matrix was found to fail first and subsequently, the loads were transferred to the other constituent phases. Along the out-of-plane transverse direction (y-direction), the CNTs reoriented along the loading direction upon polymer failure. The stacked graphene layers were found to be the major load carrying constituents along the longitudinal fiber direction (z-direction). The results of the deformation simulations indicate that the out-of-plane properties of the composite is improved by the fuzzy fiber, while the in-plane properties are maintained. The elastic material parameters along with the BDE curve can be used in a generalized method of cells (GMC) based continuum micromechanics model to define the interphase subcells surrounding the carbon fiber [30]; the damage mechanics of the fuzzy fiber nanocomposite interface at the continuum level can also be defined based on the BDE functional [36]. Furthermore, an atomistically-informed traction-separation law was also developed to define interface failure in the continuum model.

In order to isolate the effects of the polymeric surface coating, a local interphase model was developed. This local interphase containing the PSMA, an embedded CNT, and the epoxy phase were subjected to three modes of loading. The results were post-processed to isolate the cohesive forces at the interphase, and an atomistic traction-separation curve was generated for each mode of loading. These traction-separation curves were compared to those obtained for the fiber/matrix interface without the presence of the fiber surface coating. A unimodal curve represented the matrix debond mode, and trapezoidal curves were obtained for the shear-induced rotation and fiber pullout modes at the local interphase. The results showed that fuzzy fiber nanocomposites with the fiber surface coating impart enhanced out-of-plane interface properties that could delay the onset of interlaminar failure. Furthermore, the in-plane transverse properties of the interface were also improved due to the high cohesive forces between the PSMA and the epoxy, with the CNT oriented along the debond direction as a load carrying member. These results lead to a further hypothesis that a thicker layer of surface coating acting as a substrate for CNT growth, could result in higher in-plane tensile strength and out-of-plane interfacial strength. The effect of coating thickness as a variable on the cohesive behavior of the fuzzy fiber interface will be pursued as a future extension of this study. The holistic computational framework could serve as a useful tool to guide the design of nano-engineered architectures with improved performance metrics for mission-specific applications.

Acknowledgment

This research is supported by the Office of Naval Research (ONR), Grant number: N00014-17-1-2037. The program manager is Mr. William Nickerson.

References

[1] M.M. Treacy, T. Ebbesen, J. Gibson, Exceptionally high Young's modulus observed for individual carbon nanotubes, Nature 381 (No. 6584) (1996) 678–680.
[2] E.T. Thostenson, Z. Ren, T. Chou, Advances in the science and technology of carbon nanotubes and their composites: a review, Compos. Sci. Technol. 61 (No. 13) (2001) 1899–1912.
[3] Z. Hasan, A. Chattopadhyay, Y. Liu, An investigation into the performance of composite hat stringers incorporating nanocomposites using a multiscale framework, J. Reinforc. Plast. Compos. (2014), 0731684414529832.
[4] H.T. Truong, D.C. Lagoudas, O.O. Ochoa, Fracture toughness of fiber metal laminates: carbon nanotube modified Ti–polymer–matrix composite interface, J. Compos. Mater. (2013), 0021998313501923.
[5] A. Rai, A. Chattopadhyay, C. lopez, Damage analysis of various CNT architectures in nanocomposites using a multiscale approach, in: Proceedings of the American Society for Composites: Thirty-First Technical Conference, 2016. ISBN (Electronic): 20169781605953168.
[6] A. Rai, N. Subramanian, A. Chattopadhyay, Atomistically informed method of cells based multiscale approach for analysis of CFRP composites, in: ASME 2016 International Mechanical Engineering Congress and Exposition, American Society of Mechanical Engineers, 2016. V001T03A036–V001T03A036.
[7] Romanov, V.S., Lomov, S.V., Verpoest, I., "IS IT POSSIBLE TO ELIMINATE MICRO-SCALE STRESS CONCENTRATIONS IN COMPOSITES BY NANO ENGINEERING WITH CNTS?.
[8] R.D. Downes, A. Hao, J.G. Park, Geometrically constrained self-assembly and crystal packing of flattened and aligned carbon nanotubes, Carbon 93 (2015) 953–966.
[9] E.J. Siochi, J.S. Harrison, Structural nanocomposites for aerospace applications, MRS Bull. 40 (No. 10) (2015) 829–835.
[10] W. Frazier, V. Manivannan, S. Fagan, Nano-enabled Technologies for Naval Aviation Applications, 2015.
[11] D. Qian, W.K. Liu, R.S. Ruoff, Load transfer mechanism in carbon nanotube ropes, Compos. Sci. Technol. 63 (No. 11) (2003) 1561–1569.
[12] G. Chatzigeorgiou, Y. Efendiev, D.C. Lagoudas, "Homogenization of aligned "fuzzy fiber" composites, Int. J. Solid Struct. 48 (No. 19) (2011) 2668–2680.
[13] X. Ren, G.D. Seidel, Analytic and computational multi-scale micromechanics models for mechanical and electrical properties of fuzzy fiber composites, in: Proceedings paper for the 52nd AIAA/ASME/ASCE/AHS/ASC structures, structural dynamics and materials conference, Denver, Colorado, USA, 2011, pp. 4–7.
[14] S. Kundalwal, M. Ray, Effective properties of a novel continuous fuzzy-fiber reinforced composite using the method of cells and the finite element method, Eur. J. Mech. Solid. 36 (2012) 191–203.
[15] S. Lurie, D. Volkov-Bogorodskiy, O. Menshykov, Modeling the effective mechanical properties of "fuzzy fiber" composites across scales length, Compos. B Eng. (2018).
[16] S. Kundalwal, M. Ray, Thermoelastic properties of a novel fuzzy fiber-reinforced composite, J. Appl. Mech. 80 (No. 6) (2013) 061011.
[17] X. Ren, J. Burton, G.D. Seidel, Computational multiscale modeling and characterization of piezoresistivity in fuzzy fiber reinforced polymer composites, Int. J. Solid Struct. 54 (2015) 121–134.
[18] S. Kundalwal, M. Ray, Effect of carbon nanotube waviness on the effective thermoelastic properties of a novel continuous fuzzy fiber reinforced composite, Compos. B Eng. 57 (2014) 199–209.
[19] P. Miaudet, S. Badaire, M. Maugey, Hot-drawing of single and multiwall carbon nanotube fibers for high toughness and alignment, Nano Lett. 5 (No. 11) (2005) 2212–2215.
[20] B. Singh, V. Choudhary, V. Singh, Growth of carbon nanotube filaments on carbon fiber cloth by catalytic chemical vapor deposition, Appl. Nanosci. 4 (No. 8) (2014) 997–1003.
[21] N.M. O'Boyle, M. Banck, C.A. James, Open Babel: an open chemical toolbox, J. Cheminf. 3 (No. 1) (2011) 33.
[22] V. Zoete, M.A. Cuendet, A. Grosdidier, SwissParam: a fast force field generation tool for small organic molecules, J. Comput. Chem. 32 (No. 11) (2011) 2359–2368.
[23] L. Martínez, R. Andrade, E.G. Birgin, PACKMOL: a package for building initial configurations for molecular dynamics simulations, J. Comput. Chem. 30 (No. 13) (2009) 2157–2164.
[24] N. Subramanian, A. Rai, A. Chattopadhyay, Atomistically derived cohesive behavior of interphases in carbon fiber reinforced CNT nanocomposites, Carbon 117 (2017) 55–64.
[25] W.L. Jorgensen, D.S. Maxwell, J. Tirado-Rives, Development and testing of the OPLS all-atom force field on conformational energetics and properties of organic liquids, J. Am. Chem. Soc. 118 (No. 45) (1996) 11225–11236.
[26] J. Zang, Q. Yuan, F. Wang, A comparative study of Young's modulus of single-walled carbon nanotube by CPMD, MD and first principle simulations, Comput. Mater. Sci. 46 (No. 3) (2009) 621–625.
[27] T.A. Halgren, Merck molecular force field. I. Basis, form, scope, parameterization, and performance of MMFF94, J. Comput. Chem. 17 (No. 5–6) (1996) 490–519.
[28] N. Subramanian, A. Rai, A. Chattopadhyay, Atomistically informed stochastic multiscale model to predict the behavior of carbon nanotube-enhanced nanocomposites, Carbon 94 (2015) 661–672.
[29] S.K. Singh, S.G. Srinivasan, M. Neek-Amal, Thermal properties of fluorinated graphene, Phys. Rev. B 87 (No. 10) (2013) 104114.
[30] J.P. Johnston, B. Koo, N. Subramanian, Modeling the molecular structure of the carbon fiber/polymer interphase for multiscale analysis of composites, Compos. B Eng. 111 (2016) 27–36.
[31] X. Wang, J. Zhang, Z. Wang, Effects of interphase properties in unidirectional fiber reinforced composite materials, Mater. Des. 32 (No. 6) (2011) 3486–3492.
[32] Rafiee, R., and Ghorbanhosseini, A., "Predicting mechanical properties of fuzzy fiber reinforced composites: radially grown carbon nanotubes on the carbon

fiber," Int. J. Mech. Mater. Des., pp. 1–14.
[33] R. Li, N. Lachman, P. Florin, Hierarchical carbon nanotube carbon fiber unidirectional composites with preserved tensile and interfacial properties, Compos. Sci. Technol. 117 (2015) 139–145.
[34] M. Kulkarni, D. Carnahan, K. Kulkarni, Elastic response of a carbon nanotube fiber reinforced polymeric composite: a numerical and experimental study, Compos. B Eng. 41 (No. 5) (2010) 414–421.
[35] H. Shan, T. Chou, Transverse elastic moduli of unidirectional fiber composites with fiber/matrix interfacial debonding, Compos. Sci. Technol. 53 (No. 4) (1995) 383–391.
[36] N. Subramanian, B. Koo, A. Rai, Molecular dynamics-based multiscale damage initiation model for CNT/epoxy nanopolymers, J. Mater. Sci. 53 (No. 4) (2017) 2604–2617.